

## 1 Introduction

In the main paper, we present evidence for the existence of two distinct sub-populations of Be/X-ray binaries (BeXs), which are most clearly separated in the  $\log P_{\text{spin}}$  distribution. We argue that these two populations are most likely associated with different types of neutron star formation channels, with electron-capture supernovae primarily producing short- $P_{\text{spin}}$  systems, and iron-core collapse supernovae primarily producing long- $P_{\text{spin}}$  systems. This particular assignment is largely based on the eccentricity distribution of BeXs, which suggests that short- $P_{\text{spin}}$  (long- $P_{\text{spin}}$ ) systems are preferentially associated with low- $e$  (high- $e$ ) binary orbits.

Below, we provide supplementary information for several aspects of our analysis. First, we add some historical context to our discovery of two BeX sub-populations with distinct characteristic spin periods. Second, we provide additional details regarding the significance with which these sub-populations are detected in our data. Third, we discuss some subtleties regarding the interpretation of the BeX eccentricity distribution that help to properly assess the strength of the evidence for a connection between  $e$  and  $P_{\text{spin}}$ . We also show explicitly that there is no evidence for a connection between  $e$  and  $P_{\text{orb}}$ .

## 2 Historical Context

The possible existence of a gap in the distribution between  $P_{\text{spin}} \simeq 10$  s and  $P_{\text{spin}} \simeq 100$  s was actually first suggested 30 years ago, although only 10 – 20 systems were known at the time<sup>26,27</sup>. This suggestion does not seem to have been followed-up, however, perhaps because some later discoveries fell into this gap. In any case, to the best of our knowledge, the evidence for multiple sub-populations in the spin-period distribution has not been seriously reconsidered until now.

## 3 The Statistical Evidence for Two Distinct Populations of BeXs

We show in the main text that the evidence for two sub-populations contributing to the  $\log P_{\text{spin}}$  distribution of BeXs is highly statistically significant according to the standard KMM test<sup>25</sup>. The test statistic used by KMM is the likelihood ratio between the best single-Gaussian representation and the best double-Gaussian representation of the data. For the latter, we always find that the variances of the two Gaussians are consistent with each other. In our application of KMM, we thus adopt equal variances in the double Gaussian representation and then calculate the  $p$ -values robustly from bootstrap simulations<sup>28</sup>. Here and throughout this paper, the quoted  $p$ -values have the usual statistical meaning, i.e. they represent the probability of obtaining a test statistic at least as extreme as the observed one, under the assumption that the null hypothesis is correct. In the

case of KMM, the null hypothesis is that the data are drawn from a single Gaussian.

Figure 2 in the main text shows that the best double-Gaussian representation actually provides quite a good match to the  $\log P_{\text{spin}}$  data. It is nevertheless interesting to ask if we can find evidence for multiple sub-populations in our data set even without the assumption of normality. This can be checked by non-parametric methods, such as the “bandwidth test”<sup>29</sup>. The standard bandwidth test is a non-parametric test for multi-modality based on bootstrapping from a kernel density estimate of the underlying probability distribution function (PDF). The statistic used in the test is the smallest kernel width that results in a unimodal estimate of the PDF. The standard bandwidth test is a strict test of modality, in the sense that the null hypothesis is only that the underlying PDF is unimodal, with no additional assumptions concerning its shape. However, a unimodal distribution with an obvious “shoulder”, for example, may still be considered to provide strong evidence for multiple sub-populations. We can therefore also define an alternative test, in which the statistic used is the smallest kernel width that results in a kernel density estimate of the PDF that has only two inflection points<sup>30</sup>. Being entirely non-parametric, both of these tests are extremely robust. However, they are also much less powerful than KMM, mainly in the sense that their null hypotheses are so general that they are hard to rule out. The resulting  $p$ -values, which can be calibrated via Monte-Carlo simulations<sup>31</sup>, are thus always larger than those provided by KMM.

We have applied both versions of the bandwidth test to the  $P_{\text{spin}}$  data for confirmed and probable BeXs. For the standard (modality) bandwidth test, we first apply a skew-minimising Box-Cox transformation to the  $\log P_{\text{spin}}$  data, because modes associated with distinct sub-populations can be either emphasised or suppressed by certain transformations<sup>32</sup>. A transformation to symmetry is expected to make any inherent bimodality (strictly speaking: “bimodalizability”) easier to detect<sup>33</sup>. For our BeX data set, the classic bandwidth test then rejects the null hypothesis of unimodality with  $p = 9 \times 10^{-3}$  (application of this test directly to the  $\log P_{\text{spin}}$  data would give  $p = 0.04$ ). Applying the alternative (inflection point) bandwidth test directly to the  $\log P_{\text{spin}}$  data rejects the null hypothesis that there are only two inflection points in the underlying distribution with  $p = 1 \times 10^{-3}$  (application of this test to the deskewed data would give  $p = 5 \times 10^{-3}$ ). Given the robust non-parametric nature of these tests, we consider these results to be strong evidence for the existence of two distinct BeX sub-populations.

#### 4 The Eccentricity Distribution of BeXs

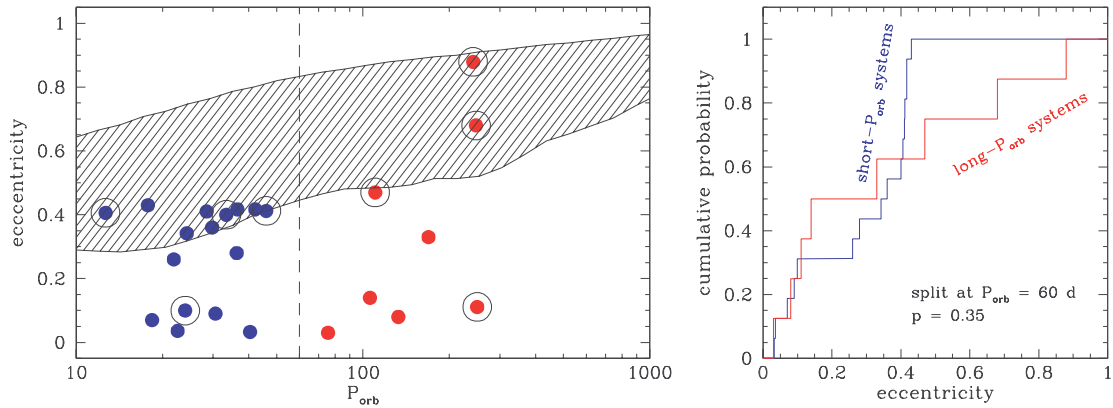
Figure 3 in the main text shows that there is marginally significant evidence that the eccentricity distribution of long- $P_{\text{spin}}$  BeXs is different from that of short- $P_{\text{spin}}$  systems. Some care has to be taken in interpreting this result.

First, tidal circularization will always tend to reduce the eccentricity of close binary systems. However, the orbital periods within our BeX sample ( $P_{\text{orb}} > 10$  d) are too long for this mechanism to be effective<sup>34</sup>. Second, other things being equal, a given supernova kick velocity will induce

larger orbital eccentricities in wide, long-period, binaries, since such systems are more weakly bound. Given that  $P_{\text{spin}}$  is correlated with  $P_{\text{orb}}$  in BeXs, this could produce a  $P_{\text{spin}} - e$  correlation in the observed sense.

Does this latter bias affect our analysis? Supplementary Figure 1 shows the  $P_{\text{orb}}$  versus  $e$  distribution for our BeX sample. Superposed on this, we also show the *predicted* location<sup>35</sup>, under the assumption that they all receive the large kicks typically associated with conventional iron-core-collapse ( $\langle v_{\text{kick}} \rangle \simeq 450 \text{ km s}^{-1}$ ). Two key conclusions may be drawn immediately from this plot. First, the observed distribution is clearly inconsistent with being drawn from a single, high-kick population. In fact, the low eccentricities ( $e \lesssim 0.4$ ) seen in many BeXs with  $P_{\text{orb}} \gtrsim 20 \text{ d}$  cannot be explained by large kicks at all. A possible connection between such low-eccentricity HMXBs<sup>36</sup> and low-kick electron capture supernovae has indeed been suggested before<sup>17,19</sup>. Second, the  $P_{\text{orb}} - e$  plane does not separate the two BeX sub-populations as cleanly as the  $P_{\text{spin}} - e$  plane. Indeed, if we split the BeX sample into short-period ( $P_{\text{orb}} < 60 \text{ d}$ ) and long-period ( $P_{\text{orb}} > 60 \text{ d}$ ) systems, their cumulative eccentricity distributions do not differ significantly ( $p = 0.35$ ). Both conclusions indicate that the link between spin period and eccentricity suggested in the main paper is not simply due to a  $P_{\text{orb}}$ -dependent bias.

Finally, there are two obvious outliers from the trend that long- $P_{\text{spin}}$  systems have preferentially high eccentricities (see Figure 3 in the main text). These systems are X Per and 1A 1118-616, which actually have the longest spin periods ( $P_{\text{spin}} = 837.7 \text{ s}$  and  $407.7 \text{ s}$ , respectively), but  $e \simeq 0.1$ . Both of these objects are known to be highly unusual within the BeX class. For example, X Per does not show the transient X-ray bursts associated with periastron passages that are the hallmark of almost all BeXs, while 1A 1118-616 is one of the furthest systems from the standard  $P_{\text{orb}} - P_{\text{spin}}$  correlation (Figure 1 of the main text). Indeed, in both systems, the dominant accretion mode probably differs from that which establishes the spin equilibrium in other BeXs<sup>37,38</sup>. This may explain why  $P_{\text{spin}}$  is *not* a valid tracer of formation channel in these two objects. Also, since 1A 1118-616 has a surprisingly short orbital period considering its slow spin ( $P_{\text{orb}} = 24 \text{ d}$ <sup>38</sup>), the low eccentricity of this system is not actually in terrible conflict with a standard (high) kick scenario<sup>35</sup>. If X Per and 1A 1118-616 are excluded from the eccentricity distribution of long- $P_{\text{spin}}$  systems, the difference to the short- $P_{\text{spin}}$  systems becomes highly significant ( $p = 0.006$ ). *A posteriori* outlier removal is, of course, a dangerous statistical practice, so this  $p$ -value cannot be taken quite at face value. Nevertheless, it is also interesting to note that all other high- $P_{\text{spin}}$  systems in Figure 3 do, in fact, lie in the region predicted for systems produced via high-kick supernovae.



**Supplementary Figure 1** The dependence of eccentricity on  $P_{\text{orb}}$  among BeXs. The left panel shows  $P_{\text{orb}}$  versus eccentricity for all confirmed and probable BeX systems with measured spin and orbital periods and eccentricities. Long- $P_{\text{spin}}$  systems with  $P_{\text{spin}} > 40$  s are additionally marked with open circles. The vertical dashed line marks the approximate division between the short- $P_{\text{orb}}$  and long- $P_{\text{orb}}$  sub-populations (see Figure 1 in the main text). The shaded area shows the region predicted to contain 60% of systems by population synthesis calculations adopting a kick velocity distribution appropriate for iron-core-collapse with mean  $\langle v_{\text{kick}} \rangle \simeq 450 \text{ km s}^{-1}$ <sup>35</sup>. The top right panel shows the cumulative eccentricity distributions of these two sub-samples. A Kolmogorov-Smirnov test provides no evidence for a significant difference between these distributions ( $p = 0.35$ ).

26. Rappaport, S. & Joss, P. C. Binary X-ray pulsars. *Nature* **266**, 123–125 (1977).
27. Bhatt, H. C. The pulse-period distribution of binary X-ray pulsars. *Astrophys. Space Sci.* **81**, 379–385 (1982).
28. Muratov, A. L. & Gnedin, O. Y. Modeling the Metallicity Distribution of Globular Clusters. *Astrophys. J.* **718**, 1266–1288 (2010). 1002.1325.
29. Silverman, B. W. Using kernel density estimates to investigate multimodality. *Journal of the Royal Statistical Society, Series B* **43**, 97–99 (1981).
30. González-Manteiga, W. & Cuevas, A. Data-driven smoothing based on convexity properties. In G. Roussas (ed.) *Nonparametric functional estimation and related topics*, vol. 335 of *NATO ASI Series C*, 225–240 (1991).
31. Hall, P. & York, M. On the calibration of Silverman’s test for multimodality. *Statistica Sinica* **11**, 515–536 (2001).

32. Knigge, C., Scaringi, S., Goad, M. R. & Cottis, C. E. The intrinsic fraction of broad-absorption line quasars. *Mon. Not. R. Astron. Soc.* **386**, 1426–1435 (2008). 0802.3697.
33. Wyszomirski, T. Detecting and displaying size bimodality: Kurtosis, skewness and bimodalizable distributions. *Journal of Theoretical Biology* **158**, 109–128 (1992).
34. North, P. & Zahn, J. Circularization in B-type eclipsing binaries in the Magellanic Clouds. *Astron. & Astrophys.* **405**, 677–684 (2003).
35. Brandt, N. & Podsiadlowski, P. The effects of high-velocity supernova kicks on the orbital properties and sky distributions of neutron-star binaries. *Mon. Not. R. Astron. Soc.* **274**, 461–484 (1995).
36. Pfahl, E., Rappaport, S., Podsiadlowski, P. & Spruit, H. A New Class of High-Mass X-Ray Binaries: Implications for Core Collapse and Neutron Star Recoil. *Astrophys. J.* **574**, 364–376 (2002).
37. Delgado-Martí, H., Levine, A. M., Pfahl, E. & Rappaport, S. A. The Orbit of X Persei and Its Neutron Star Companion. *Astrophys. J.* **546**, 455–468 (2001). [arXiv:astro-ph/0004258](https://arxiv.org/abs/astro-ph/0004258).
38. Staubert, R. *et al.* Finding a 24-day orbital period for the X-ray binary 1A 1118-616. *Astron. & Astrophys.* **527**, A7+ (2011). 1012.2459.